Thermal Degradation Kinetics of Poly(*N*-adamantyl-*exo*-nadimide) Synthesized by Addition Polymerization

Binyuan Liu, Yang Li, Li Zhang, Weidong Yan, Shuhuan Yao

Institute of Polymer Science and Engineering, School of Chemical Engineering, Hebei University of Technology, Tianjin, 300130, China

Received 2 June 2006; accepted 10 August 2006
DOI 10.1002/app.25422
Published online in Wiley InterScience (www.interscience.wiley.com).

ABSTRACT: The thermal decomposition behavior and degradation kinetics of poly(*N*-adamantyl-*exo*-nadimide) were investigated with thermogravimetric analysis under dynamic conditions at five different heating rates: 10, 15, 20, 25, and 30°C/min. The derivative thermogravimetry curves of poly (*N*-adamantyl-*exo*-nadimide) showed that its thermal degradation process had one weight-loss step. The apparent activation energy of poly(*N*-adamantyl-*exo*-nadimide) was estimated to be about 214.4 kJ/mol with the Ozawa–Flynn–Wall method. The most likely decomposition process was an F1 deceleration type in terms of the Coats–Redfern and Phadnis–Deshpande results. © 2006 Wiley Periodicals, Inc. J Appl Polym Sci 103: 3003–3009, 2007

Key words: activation energy; thermal properties; thermogravimetric analysis (TGA)

INTRODUCTION

Vinyl-type polynorbornene (PNB) exhibits many key properties, such as high thermal stability, high optical transparency, a high refractive index, low birefringence, and a low dielectric constant. PNB thus has potential applications in microelectronic, optical, and semiconductor devices.[1–5] However, pure PNB exhibits insufficient adhesion to substrates with polar surfaces such as silicon, oxides, and metals.[6] In addition, the rigid backbone results in a rather brittle material with a very low elongation at break.[3–5] To overcome these shortcomings, a functional group such alkoxysilyl, alkyl, or ester can be incorporated into the backbone of PNB. Although these groups can enhance the adhesion to surfaces and improve the elongation at break and solubility in common solvents such as tetrahydrofuran, chloroform, and acetone,[5,7–12] in general, the glass-transition temperatures and thermal stabilities of these materials are reduced versus those of nonfunctionalized PNB.[5] Heitz and coworkers[13] reported the synthesis of vinyl-type poly(*N*-tolyl nadimide)s with a Pd(II) catalyst in 1999, and the results showed that the imide group incorporated into the PNB backbone improved its solubility and maintained high thermal stability in comparison with the parent PNB.

Thermogravimetric analysis (TGA) has come into wide use in the last decades for rapidly assessing the thermal stability of various substances, including polymer pyrolyses.[14] The kinetic parameters of degradation processes, such as the rate constants, activation energies, reaction orders, and Arrhenius preexponential factors, can be assessed in light of data recorded from thermograms. Many kinetic analytical methods have been established on the basis of the scanning-rate dependence of TGA data.[15–17]

In this study, a new kind of polynadimide, poly (*N*-adamantyl-*exo*-nadimide) [poly(*N*-AdNDI)], showing good thermal stability and solubility comparable to those of poly(*N*-tolyl nadimide)s,[13] was synthesized by vinyl-type polymerization, and its thermal stability was investigated with TGA under dynamic conditions. Here two aspects were concerned. One was the thermal degradation behavior of poly(*N*-AdNDI), including the effect of the heating rate on the degradation temperature and weight-loss percentage; the other was the kinetics of the thermal degradation mechanism and the apparent activation energy of poly(*N*-AdNDI).

THEORETICAL[15–19]

In the general reaction, $B(s) \rightarrow D(s) + C(g)$. The disappearance rate (B) can be determined as follows:

$$\frac{da}{dt} = kf(a) \tag{1}$$

where $B(s)$ is the reactant, $D(s)$ and $C(g)$ are the remainder and gasous production, a is the extent of conversion of B decomposed at time t and k is the

Correspondence to: B. Liu (byliu@hebut.edu.cn).

Contract grant sponsor: National Natural Science Foundation; contract grant number: 50403013.

Contract grant sponsor: Scientific Research Foundation for Returned Overseas Chinese Scholars of the State Education Ministry.

rate constant. k is assumed to obey an Arrhenius relationship for the beginning of the reaction:

$$k = A\exp(-E/RT) \tag{2}$$

where A is the frequency factor or pre-exponential factor, R is the gas constant, T is absolute temperature and E is the activation energy of the reaction. Combining eqs. (2) and (1) gives the following relationship:

$$\frac{da}{dt} = A\exp(-E/RT)f(a) \tag{3}$$

If the temperature of the sample is changed by a controlled and constant heating rate ($\varphi = dT/dt$), the variation in the degree of conversion can be analyzed as a function of temperature, this temperature depending on the time of heating. Hence, the reaction rate is defined as follows:

$$\frac{da}{dt} = (A/\varphi)\exp(-E/RT)f(a) \tag{4}$$

Separating the variable and rearranging and integrating eq. (4), we can write the equation as follows:

$$g(a) = \int_{a_o}^{a_p}\frac{da}{f(a)} = \frac{A}{\varphi}\int_{T_o}^{T_p}\exp(-E/RT)dT \tag{5}$$

where $g(a)$ is a function of the conversion, a_o and a_p are reactant conversion at point o and p, T_o and T_p are corresponding to temperature point o and p, respectively. If we define x as equal to E/RT and integrate the right-hand side of eq. (5), we obtain the following equation:

$$\frac{A}{\varphi}\int_{To}^{Tp}\exp(-E/RT)dT = \frac{AE}{\varphi T}p(x) \tag{6}$$

After taking the logarithms, we have

$$\log\varphi = \log\frac{AE}{g(a)R} + log\ p(x) \tag{7}$$

where

$$p(x) = \frac{e^{-x}}{x^2}\sum_{n=1}(-1)^{n-1}\frac{n!}{x^{n-1}} \tag{8}$$

The function $p(x)$ can be expressed by some approximate equation when certain conditions are met. The methods studied in this article are as follows.

Ozawa–Flynn–Wall method[15]

This is one of the integral methods that can determine the activation energy without knowledge of the reaction order; it is essentially the same as the Flynn–Wall method, representing a relatively simply method for determining the activation energy directly from data of the weight loss versus the temperature obtained at several heating rates. Equation (7) is integrated with Doyle's approximation;[18] that is, when $20 \le x \le 60$, the function $p(x)$ can be adapted to the following approximation:

$$\log p(x) \approx -2.315 - 0.4567x \tag{9}$$

Substituting eq. (9) into eq. (7), we obtain the following result of the integration after taking logarithms:

$$\log\varphi = \log\frac{AE}{g(a)R} - 2.315 - \frac{0.4567E}{RT} \tag{10}$$

where φ, A, E, and T have the known meanings and $g(\alpha)$ is the integral function of conversion. Thus, at the given conversion, a plot of $\log\varphi$ against $1/T$ should be a straight line with a slope of $-0.4567E/R$.

Coats–Redfern method[16]

Coats and Redfern[16] used an asymptotic approximation for the resolution of eq. (5) at different conversion values. If we suppose that $(2RT)/E \to 0$ for the Doyle approximation,[18] we finally obtain the following in a natural logarithmic form:

$$\ln\frac{g(a)}{T^2} = \ln\frac{AR}{\varphi E} - \frac{E}{RT} \tag{11}$$

According to the theoretical functions of $g(a)$ for the different degradation processes listed in Table I,[20] we can not only obtain the apparent activity energy and frequency factor from the slope of the plot of $\ln(g(a))/T^2$ versus $1/T$ but also learn the valid reaction mechanism.

Phadnis–Deshpande method[17]

When taking the function $p(x)$ for the two former terms, we can express eq. (7) as follows:

$$g(a) = \frac{ART^2}{\varphi E}\left[1 - \frac{2RT}{E}\right]\exp(-E/RT) \tag{12}$$

Rewriting eq. (12) by substituting eq. (4) and rearranging it, we obtain the following:

$$f(a)g(a) = \frac{RT^2}{E}\left[1 - \frac{2RT}{E}\right]\frac{da}{dT} \tag{13}$$

When we pass over the comparatively small term $2R^2T^3/E^2$, eq. (13) shortens to

$$f(a)g(a) = \frac{RT^2}{E}\frac{da}{dT} \tag{14}$$

TABLE I
Algebraic Expressions for $g(a)$ for the Most Frequently Used Mechanisms of Solid-State Processes

Symbol	$g(a)$	Solid-state process
Sigmoidal curves		
A2	$[-\ln(1-a)]^{1/2}$	Nucleation and growth [Avrami–Erofeev eq. (1)]
A3	$[-\ln(1-a)]^{1/3}$	Nucleation and growth [Avrami–Erofeev eq. (2)]
A4	$[-\ln(1-a)]^{1/4}$	Nucleation and growth [Avrami–Erofeev eq. (3)]
Deceleration curves		
R1	a	Phase-boundary-controlled reaction (one-dimensional movement)
R2	$2[1-\ln(1-a)^{1/2}$	Phase-boundary-controlled reaction (contracting area)
R3	$3[1-\ln(1-a)^{1/3}$	Phase-boundary-controlled reaction (contracting volume)
D1	a^2	One-dimensional diffusion
D2	$(1-a)\ln(1-a)+a$	Two-dimensional diffusion (Valensi equation)
D3	$[1-(1-a)^{1/3}]^2$	Three-dimensional diffusion (Jander equation)
D4	$(1-\frac{2}{3}a)-(1-a)^{2/3}$	Three-dimensional diffusion (Ginstling–Brounshtein equation)
F1	$-\ln(1-a)$	Random nucleation with one nucleus on the individual particle
F2	$\frac{1}{(1-a)}$	Random nucleation with two nuclei on the individual particle
F3	$\frac{1}{(1-a)^2}$	Random nucleation with two nuclei on the individual particle

The information presented in this table was taken from refs. 20 and 21.

Alternatively, upon the integration of eq. (14), we have the following expression:

$$g'(a) = -\frac{E}{RT} \tag{15}$$

where $g'(a) = \int f(a)g(a)da$. The integral functions of $g'(a)$ are listed in Table II.

This method can deduce the reaction mechanism depending on the functional form of a, based on the linearity of the plot of $f(a)$, $g(a)$ versus T^2da/dT or $g'(a)$ versus $1/T$, and the apparent activity energy, which is obtained by other methods (e.g., Ozawa–Flynn–Wall methods). The plot of $g'(a)$ versus $1/T$ is linear with the proper functional form of a. The slope of this plot, if multiplied by R, gives the value of E. The application of this method, like the Coats–Redfern method, gives a means of acquiring the valid reaction mechanism. In the case of polymers, the integral function, $g(a)$, is a form of either a sigmoidal function or a deceleration function. Table I presents different expressions of $g(a)$ for the different solid-state mechanisms.[20,21] These functions usually estimated the solid-state mechanism of the reaction from nonisothermal TGA experiments.

EXPERIMENTAL

Poly(*N*-AdNDI) was synthesized by addition polymerization with a Pd(II) complex as the catalyst.[13] The Fourier transform infrared transmission spectra were obtained on a Vector 22 spectrometer with KBr pellets for compound I from 400 to 4000 cm^{-1} at a resolution of 4 cm^{-1} (16 scans collected). ^{1}H-NMR analyses were performed on a Varian Mercury 300 spectrometer (Bruker, Germany) (300 MHz) with $CDCl_3$ as the solvent. The chemical shifts are reported as parts per million with tetramethylsilane as the internal reference; TGA was performed with a TA 2960 instrument. The polymer sample (6.0 ± 0.5 mg) was stacked in an open platinum sample pan, and the experiment was conducted under a nitrogen gas atmosphere, the flowing rate of which was 80 mL/min, at various heating rates (10, 15, 20, 25, and 30°C/min) in the range of 50–750°C.

RESULTS AND DISCUSSION

Figure 1 presents the ^{1}H-NMR spectrum of poly (*N*-AdNDI). The monomer olefin signal at δ = 6.28 ppm has disappeared. Meanwhile, the ^{1}H-NMR spectrum does not show a vinyl proton in the range of 5.0–6.0 ppm for the polymer, and this corresponds to double bonds of the polymer obtained by ring-opening metathesis polymerization,[22(a)] indicating polymerization through a vinyl-type mechanism rather than ring-opening metathesis polymerization. The IR spectrum

TABLE II
Functions of $g'(a)$ for Frequently Used Solid-State Reaction Mechanisms in the Phadnis–Deshpande Method[17]

$g'(a)$	Reaction mechanism
$\ln a$	Power law
$2\ln a$	Power law
$\ln[1-(1-a)^{1/3}]$	Phase boundary (contracting sphere)
$\ln[1-(1-a)^{1/2}]$	Phase boundary (contracting cylinder)
$\frac{1}{2}\ln[-\ln(1-a)]$	Nucleation and nucleus growth (Avrami–Erofeev nucleus growth)
$\frac{1}{3}\ln[-\ln(1-a)]$	Nucleation and nucleus growth (Avrami–Erofeev nucleus growth)
$\frac{1}{4}\ln[-\ln(1-a)]$	Nucleation and nucleus growth (Avrami–Erofeev nucleus growth)
$\ln[(1-a)\ln(1-a)+a]$	Valensi two-dimensional diffusion
$2\ln[1-(1-a)^{1/3}]$	Jander three-dimensional diffusion
$\ln[1-\frac{2}{3}a-(1-a)^{2/3}]$	Brounshtein–Ginstling three-dimensional diffusion

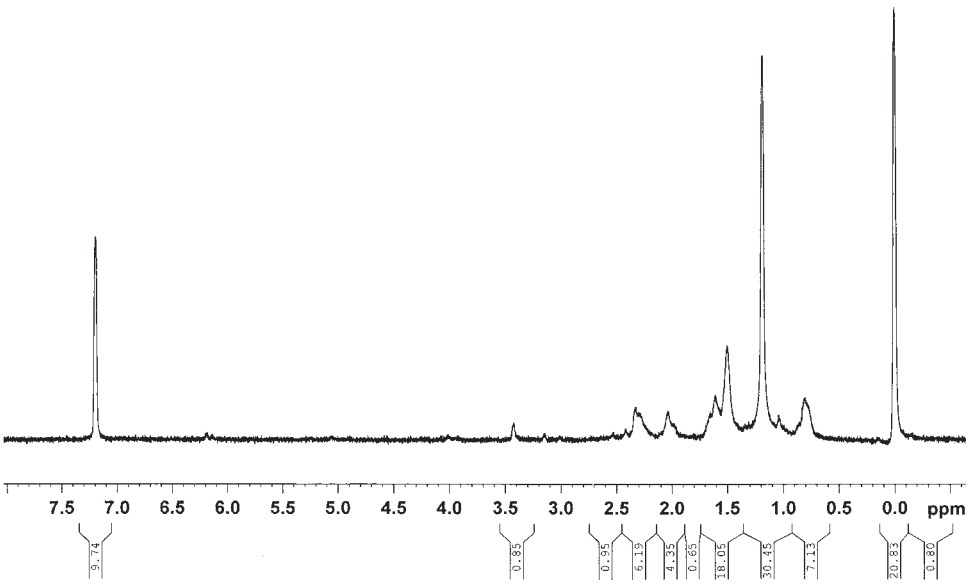

Figure 1 ^{1}H-NMR spectrum of poly(*N*-AdNDI).

agrees with the fact that the obtained polymers occur through vinyl-type polymerization. The peak at 3045 cm^{-1}, characteristic of the C—H stretching vibration of C=C—H, which is in the presence of the monomer, has disappeared in the IR spectrum of the resulting polymer (see Fig. 2). In comparison with the monomer, there is also no absorption at 1665 or 784 cm^{-1}, which is characteristic of the C=C double bond in the resulting copolymer. However, the characteristic absorption peak signal for the C—C bond of the norbornene ring at 975 cm^{-1} still exists before and after polymerization.[22(b)] Poly(*N*-AdNDI), comparable to poly(*N*-tolyl nadimide)s, shows good solubility in common organic solvents, such as tetrahydrofuran, chloroform, and toluene, whereas pure PNB is insoluble in these solvents. Detailed polymerizations will be reported in another publication.

The TGA and derivative thermogravimetry (DTG) curves for the pyrolysis of poly(*N*-AdNDI) are shown in Figure 3(a,b), respectively. The TGA thermograms, obtained from nitrogen-purged samples, shift toward the high-temperature zone as the heating rate increases from 10 to 30°C/min because of the heat lag of the process.[14] This heating-rate dependence is also indicated in the DTG thermograms. That is, the peak of the DTG thermogram shifts to higher temperatures as the heating rate increases. The DTG curves [Fig. 2(b)] show only a maximum weight-loss-rate peak, and this indicates that the decomposition corresponds to a single-stage decomposition reaction in which the decomposition temperatures are well defined. The decomposition behaviors at all heating rates are analogous to one another at different heating rates, as indicated in Figure 3(b).

Figure 4 presents the influence of the heating rate on the decomposition temperature. The temperature at the onset of weight loss (T_i) and the temperature of the final decomposition (T_f) were obtained from the TGA curve with the tangent method, whereas the temperature at the maximum weight-loss rate (T_p) was taken from DTG curves. Figure 3 shows that the thermal degradation temperature increases with the heating rate. The relationships between the decomposition temperatures and heating rate are as follows:

$$T_i = 735.3 + 0.80\varphi$$

$$T_p = 756.1 + 0.77\varphi$$

$$T_f = 771.5 + 0.83\varphi$$

When the heating rate is approximately zero, the corresponding decomposition temperature can be expressed more exactly as an equilibrium decompo-

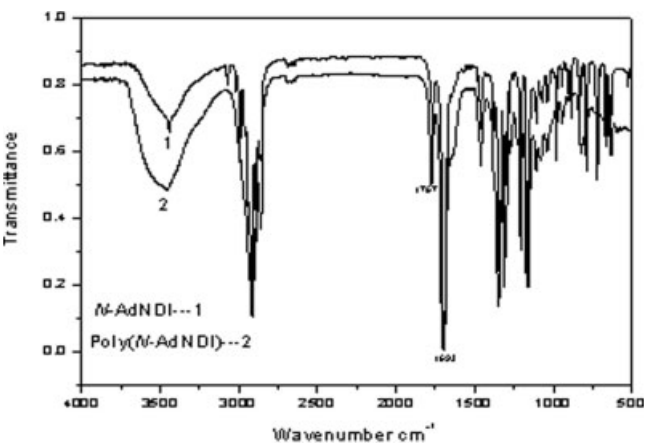

Figure 2 IR spectra of monomer *N*-adamantyl-*exo*-nadimide (*N*-AdNDI) and poly(*N*-AdNDI).

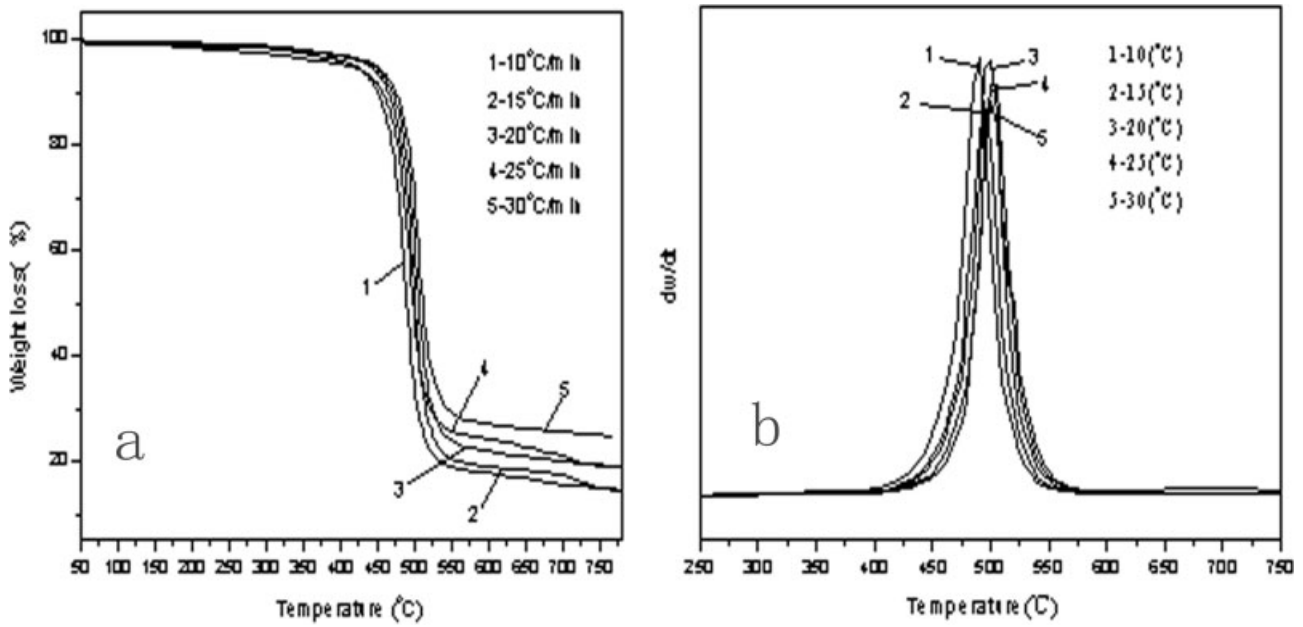

Figure 3 (a) TGA and (b) DTG curves of poly(*N*-AdNDI) thermal degradation at different heating rates.

sition temperature.[23] The equilibrium values of T_i, T_p, and T_f are 735.3, 756.1, and 771.5 K, respectively, for poly(*N*-AdNDI).

Kinetic analysis

Evaluation of the activation energy

The calculations of the Ozawa–Flynn–Wall method[15] are applicable to all points on the TGA curves, so they are capable of providing reasonably reliable data. We used the Ozawa–Flynn–Wall method to calculate the activation energy for the decomposition of a poly(*N*-AdNDI) system with different conversion values by fitting the plots of log ϕ versus 10,000/T, as shown in Figure 5. From the slopes of the plots, the apparent activation energy, E, can be calculated:

$$E = -\text{Slope} \times R/0.4567$$

Figure 3 shows that the fitted straight lines are nearly parallel, thus indicating the applicability of this method to our system in the conversion range studied (from 10 to 26%). Table III shows the activation energies corresponding to different conversions. From these values, a mean value of 214.4 kJ/mol has been

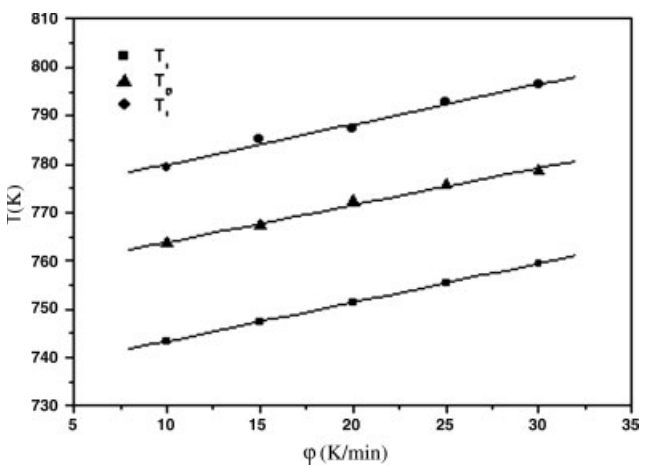

Figure 4 Relationship between the thermal decomposition temperatures and φ for poly(*N*-AdNDI): (●) T_f, (▲) T_p, and (■) T_i.

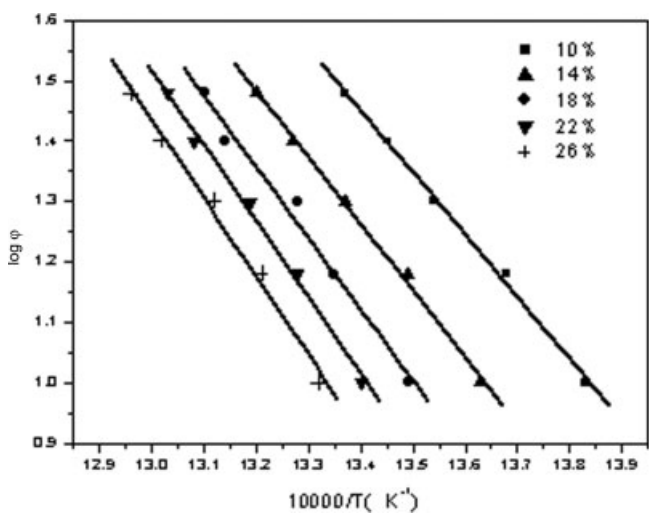

Figure 5 Typical plots of log φ versus 10,000/T at several conversions in the range of 10–26% in steps of 4% (the Ozawa–Flynn–Wall method).

TABLE III
Values of *E* obtained with the Ozawa–Flynn–Wall Method

a (%)	*E* (kJ/mol)	*R*[a]
10	187.1	0.9958
14	199.6	0.9986
18	215.7	0.9915
22	232.6	0.9941
26	237.1	0.9956

[a] Correlation coefficient.

obtained. This method has the advantage of not needing previous knowledge of the reaction mechanism to solve the activation energy. Therefore, some authors[24,25] have used the activation energies obtained with this method to validate their thermal degradation mechanism models.

Kinetic analysis evaluation of the thermal degradation mechanism

Many mathematical methods have been postulated in the literature[20,21] for the affirmation of the mechanism of a solid-state reaction from thermoanalytical curves obtained isothermally or nonisothermally. In general, the correlation coefficient of plots for different mechanism functions has been regarded as a standard for determining the reaction mechanism, but sometimes the correlation coefficients of the lines have slight differences; in this case, it is necessary to determine the mechanism in terms of other supplementary methods.[26] We use the Coats–Redfern method and Phadnis–Deshpande method to investigate the model for poly(*N*-AdNDI) decomposition by comparing the activation energy values with the calculations of the Ozawa–Flynn–Wall method, except by way of the relative linearity of the plot.

The apparent activation energy corresponding to different $g(a)$ values for sigmoidal and decelerated mechanisms (Table I) can be obtained at constant heating rates with the Coats–Redfern equation from a fitting of plots of $\ln(g(a))/T^2$ versus $10{,}000/T$. Table IV shows the activity energies and correlations at a heating rate of 20°C/min. The linearity of plots $\ln(g(a))/T^2$ versus $10{,}000/T$ for R2, R3, F2, and F3 types was bad. Therefore, when we looked at the correlation coefficient (good linearity of the plot) as the standard, R2, R3, F2, and F3 types of degradation processes were excluded first. In addition, a comparison of the values of the activation energy in Table IV shows that at a heating rate of 20°C/min, the apparent activation energies are in good agreement with those obtained with the Ozawa–Flynn–Wall method with the R1 and F1 mechanisms, that is, a phase-boundary-controlled reaction (one-dimensional movement) and random nucleation with one nucleus on the individual particle, respectively.

TABLE IV
Values of *E* Obtained with the Coats–Redfern Method for Several Solid-State Processes at a Heating Rate of 20 °C/min

Mechanism	*E* (kJ/mol)	*R*[a]
A2	103.9	0.9971
A3	65.2	0.9971
A4	47.3	0.9994
R1	209.0	0.9990
R2	6.9	0.9229
R3	20.1	0.9874
D1	416.5	0.9990
D2	134.3	0.9953
D3	444.9	0.9986
D4	435.9	0.9989
F1	222.8	0.9982
F2	30.7	0.9718
F3	73.2	0.9768

[a] Correlation coefficient.

To further confirm the thermal degradation behavior, we also calculated the apparent activation energies via the Phadnis–Deshpande method in its integral form at a heating rate of 20°C/min. The values of the activation energies according to this method are listed in Table V. The correlations of all the plots were good, but only when the thermal process abided by a power law and phase boundary (see entries 1 and 4 in Table II), whose values of the apparent activation energy of poly(*N*-AdNDI) degradation were close to those from the Ozawa–Flynn–Wall method. With the combination of the Coats–Redfern and Phadnis–Deshpande results, the more possible mechanism of poly(*N*-AdNDI) degradation was a phase boundary.

TABLE V
Values of *E* Obtained with the Phadnis–Deshpande Method for Solid-State Processes at a Heating Rate of 20 °C/min

Reaction mechanism	*E* (kJ/mol)	*R*[a]
Power law	214.7	0.9991
Power law	429.3	0.9991
Phase boundary	230.3	0.9987
Phase boundary	224.4	0.9989
Nucleation and growth [Avrami eq. (1)]	119.1	0.9988
Nucleation and growth [Avrami eq. (2)]	78.0	0.9987
Nucleation and growth [Avrami eq. (3)]	59.4	0.9988
Valensi two-dimensional diffusion	414.7	0.9960
Jander three-dimensional diffusion	456.6	0.9986
Brounshtein–Ginstling three-dimensional diffusion	464.4	0.9820

[a] Correlation coefficient.

CONCLUSIONS

The thermal degradation behavior and apparent activation energy of poly(*N*-AdNDI) were studied with TGA and DTG. The results revealed that the thermal degradation of poly(*N*-AdNDI) involved a single weight-loss step. The apparent activation energy of the thermal degradation of poly(*N*-AdNDI) calculated with the Ozawa–Flynn–Wall method was 214.4 kJ/mol. The most possible decomposition process was an F1 deceleration type according to the Coats–Redfern and Phadnis–Deshpande methods.

References

1. Peters, L. Semicond Int 2001, 24, 66.
2. Okoroanyanwu, U.; Shimokawa, T.; Byers, J.; Willson, C. G. Chem Mater 1998, 10, 3319.
3. Chiniwalla, P.; Bai, Y.; Elce, E.; Shick, R. A.; Allen, S. A.; Kohl, P. A. J Appl Polym Sci 2004, 91, 1020.
4. Haselwander, T. F. A.; Heitz, W.; Krugel, S. A.; Wendorff, J. H. Macromolecules 1997, 30, 5345.
5. (a) Grove, N. R.; Kohl, P. A.; Allen, S. A. B.; Saikumar, J.; Shick, R. J Polym Sci Part B: Polym Phys 1999, 37, 3003–10; (b) Müller, K; Kreiling, S.; Dehnicke, K.; Allgaier, J.; Richter, D.; Fetters, L. J.; Jung, Y. S.; Yoon, D. Y.; Greiner, A. Macromol Chem Phys 2006, 207, 193.
6. Pasquale, A. J.; Truong, H. D.; Allen, R. D.; Long, T. E. Polym Prepr 2001, 41, 302.
7. Shin, B. G.; Jang, M. S.; Yoon, D. Y.; Heitz, W. Macromol Rapid Commun 2004, 25, 728.
8. Byun, G. S.; Kim, S. Y.; Cho, I. J Polym Sci Part A: Polym Chem 2006, 44, 1263.
9. Mathew, J. C.; Reinmuth, A.; Melia, J.; Swords, N.; Risse, W. Macromolecules 1996, 29, 2755.
10. Goodall, B. L.; Risse, W.; Mathew, J. C. PCT Int. App. WO 9637526 (1996).
11. Heinz, B. S.; Heitz, W.; Krügel, S. A.; Raubacher, F.; Wendorff, J. H. Acta Polym 1997, 48, 385.
12. Myagmarsuren, G.; Lee, K. S.; Jeong, O. Y.; Ihm, S. K. Polymer 2005, 46, 3685.
13. Heitz, W.; Krüger, S. A.; Madam, R.; Wendorff, J. H. Macromol Chem Phys 1999, 200, 338.
14. Li, L. Q.; Guan, C. X.; Zhang, A. Q.; Chen, D. H.; Qing, Z. B. Polym Degrad Stab 2004, 84, 369.
15. Ozawa, T. Bull Chem Soc Jpn 1965, 38, 1881.
16. Coats, A. W.; Redfern, J. P. Nature 1964, 201, 68.
17. Phadnis, A. B.; Deshpande, V. V. Thermochim Acta 1983, 62, 361.
18. Doyle, C. D. J Appl Polym Sci 1961, 5, 285.
19. Thermal Analysis Kinetics; Hu, R. Z.; Shi, Q. Z., Eds.; Science: Beijing 2001; p 127.
20. Fraga, F.; Rodríguez-Núñez, E. J Appl Polym Sci 2001, 80, 776.
21. Thermal Analysis—Techniques & Applications; Charsky, E. L.; Warrington, S. B., Eds.; Royal Society of Chemistry: London, 1992; p 52.
22. (a) Bazan, G. C.; Schrock, R. R.; Cho, H. N.; Gibson, V. C. Macromolecules 1991, 24, 4495–4502; (b) Contreras, A P.; Cerda, A. M.; Tlenkopatchev, M. Macromol Chem Phys 2002, 203, 1811.
23. Li, S. D.; Yu, P. H.; Cheung, M. K. J Appl Polym Sci 2001, 80, 2237.
24. Núñez, L.; Fraga, F.; Núñez, M. R.; Castro, A.; Fraga, L. J Appl Polym Sci 1999, 74, 2997.
25. Montserrat, S.; Málek, J.; Colomer, P. Thermochim Acta 1998, 313, 83.
26. Straszko, J.; Olszak-Humienik, M.; Mozejko, J. Thermochim Acta 1997, 292, 145.